

Bridging constrained random-phase approximation and linear response theory for computing Hubbard parameters

Alberto Carta,^{1,*} Iurii Timrov,^{2,†} Sophie Beck,³ and Claude Ederer^{1,‡}

¹*Materials Theory, ETH Zürich, Wolfgang-Pauli-Strasse 27, 8093 Zürich, Switzerland*

²*PSI Center for Scientific Computing, Theory, and Data, 5232 Villigen PSI, Switzerland*

³*Center for Computational Quantum Physics, Flatiron Institute, 162 5th Avenue, New York, NY 10010, USA*

(Dated: May 7, 2025)

The predictive accuracy of popular extensions to density-functional theory (DFT) such as DFT+ U and DFT plus dynamical mean-field theory (DFT+DMFT) hinges on using realistic values for the screened Coulomb interaction U . Here, we present a systematic comparison of the two most widely used approaches to compute this parameter, linear response theory (LRT) and the constrained random-phase approximation (cRPA), using a unified framework based on the use of maximally localized Wannier functions to define the underlying basis sets. We demonstrate good quantitative agreement between LRT and cRPA in cases where the strongly interacting subspace corresponds to an isolated set of bands. Differences can be assigned to neglecting the response of the exchange-correlation potential in cRPA and the presence of additional screening channels in LRT. Moreover, we show that in cases with strong hybridization between interacting and screening subspaces, the application of cRPA becomes ambiguous and can lead to unrealistically small U values, while LRT remains well-behaved. Our work clarifies the relation between both methods, sheds light on their strengths and limitations, and emphasizes the importance of using a consistent set of Wannier orbitals to ensure transferability of U values between different implementations.

An accurate description of many quantum materials [1] relies on correctly capturing the strong electron-electron interaction among a subset of electrons inhabiting the states around the Fermi level. The method of choice is to divide the electrons into strongly and weakly interacting subspaces, where the latter can be treated within common approximations to density-functional theory (DFT) [2, 3], while the strongly interacting subspace is augmented with a more accurate treatment of the local electron-electron interaction, resulting in the widely used DFT+ U [4–7] or DFT plus dynamical mean-field theory (DFT+DMFT) methods [8–10].

The accuracy and predictive capabilities of these techniques depend on a realistic estimation of the screened Coulomb interaction within the strongly interacting subspace, which is typically parametrized in terms of an on-site Hubbard U (and potentially an on-site Hund’s coupling J [5] and/or an inter-site interaction [11]). Consequently, several first-principles approaches to compute Hubbard parameters have been developed, including constrained DFT [12–20], linear response theory (LRT) [21–26], Hartree-Fock-based methods [27–32], and the constrained random-phase approximation (cRPA) [33–36]. In particular, LRT and cRPA are widely used in practical applications. Notably, LRT is used almost exclusively for DFT+ U calculations, in particular for high-throughput applications of DFT+ U [7, 37–39], while cRPA is utilized more often in the context of DFT+DMFT calculations [40–42].

This raises the question to what extent LRT and cRPA

can be viewed as equivalent. While some attempts were made to compare different methods for computing Hubbard parameters [36, 43, 44], there is still lack of understanding and consensus regarding the similarities and differences between them. So far, an explicit quantitative comparison of the calculated U parameters has been hindered by the fact that specific implementations generally use different basis orbitals to represent the strongly interacting subspace, with the U parameter depending very sensitively on the specific choice of these orbitals [7, 37, 45, 46]. Many DFT codes implementing the LRT method use internally defined localized orbitals (e.g., orthogonalized atomic orbitals [45] or partial wave projectors [47]), while cRPA calculations are often based on Wannier functions [48–51].

In this letter, we systematically compare U values obtained from LRT and cRPA. We specifically address the need for a consistent definition of the interacting subspace and a consistent choice of *Hubbard projectors*, which represent the corresponding localized basis orbitals. To this end, we extend the LRT calculation of the U parameter using density-functional perturbation theory [22, 24] within QUANTUM ESPRESSO [52–54] by interfacing it with WANNIER90 [55] in order to employ maximally localized Wannier functions (MLWFs) [56] as Hubbard projectors. This enables a direct quantitative comparison between LRT and cRPA, the latter being evaluated using QUANTUM ESPRESSO in combination with RESPACK [57, 58]. We demonstrate that, for cases where the division of the interacting and screening subspaces corresponds to isolated or nearly-isolated sets of bands, LRT and cRPA yield remarkably similar results. However, we also show that the two approaches are not strictly equivalent and identify the corresponding differences. For cases where the two subspaces hybridize

* alberto.carta@mat.ethz.ch

† iurii.timrov@psi.ch

‡ edererc@ethz.ch

strongly, the application of cRPA becomes problematic, leading to unrealistically small U values, whereas LRT remains largely unaffected.

We begin by briefly summarizing the basic terminology of both approaches. An essential quantity in both methods is the charge susceptibility, or *response tensor*, which characterizes how a system of interacting electrons reacts to external perturbations. Thereby, one distinguishes between the *bare* susceptibility, χ_0 , which does not consider the change in the electronic interactions caused by the charge rearrangement, and the *full* susceptibility, χ , which considers both the external perturbation and the effect of the resulting electron redistribution.

In LRT, these susceptibilities are obtained by directly calculating the response of the Kohn-Sham (KS) system to small perturbations, with $\tilde{\chi}^{IJ} = \partial n^I / \partial \lambda^J$ defined as change in occupation of the Hubbard projector orbitals on site I due to a local potential shift on site J , λ^J , acting only within the interacting subspace. The Hubbard parameter for site I is then defined as the corresponding diagonal element of the difference of the inverse susceptibility matrices [7, 21]:

$$U_{\text{LRT}}^I = (\tilde{\chi}_0^{-1} - \tilde{\chi}^{-1})^{II}, \quad (1)$$

where $\tilde{\chi}_0$ is calculated without considering the change in the KS potential resulting from the charge rearrangement. Note that here the tilde indicates that the corresponding susceptibilities only describe the ‘‘coarse grained’’ density response on a per site basis.

The cRPA formalism [35, 36] emphasizes the division of the electronic Hilbert space into the *interacting subspace*, \mathcal{D} , (also called ‘‘target’’ subspace or ‘‘correlated’’ subspace in the context of DFT+DMFT) and the *screening subspace* (also called ‘‘rest’’ subspace), mirroring the corresponding division within DFT+ U and DFT+DMFT.¹ Within RPA, the bare susceptibility can be written as a sum over all possible particle-hole excitations in an independent particle basis:

$$\chi_0(\omega, \mathbf{r}, \mathbf{r}') = \sum_{m,n} \frac{f_n - f_m}{\omega + \epsilon_n - \epsilon_m} \langle \mathbf{r} | \psi_m \rangle \langle \psi_n | \mathbf{r} \rangle \langle \mathbf{r}' | \psi_n \rangle \langle \psi_m | \mathbf{r}' \rangle, \quad (2)$$

where $|\psi_n\rangle$, ϵ_n , and f_n are the KS states, their energies, and occupations, respectively. One can split the bare susceptibility into two parts, $\chi_0 = \chi_0^{\mathcal{D}} + \chi_0^{\mathcal{R}}$, where $\chi_0^{\mathcal{D}}$ contains only particle-hole excitations within the interacting subspace, and $\chi_0^{\mathcal{R}}$ contains all other transitions. The partially screened Coulomb interaction acting within the \mathcal{D} subspace is then obtained as $W^{\mathcal{R}} = [1 - V\chi_0^{\mathcal{R}}]^{-1}V$, where $V = 1/|\mathbf{r} - \mathbf{r}'|$ is the unscreened Coulomb interaction. Static interaction parameters are computed as

matrix elements of $W^{\mathcal{R}}(\omega = 0)$ with the Hubbard projector functions $\phi_i^I(\mathbf{r})$, *i.e.*, the specific basis orbitals used to represent \mathcal{D} , corresponding to orbital i on site I [35]:

$$(W^{\mathcal{R}})_{ijkl}^{IJKL} = \int \int \phi_i^I(\mathbf{r})^* \phi_j^J(\mathbf{r}) \times W^{\mathcal{R}}(\omega = 0, \mathbf{r}, \mathbf{r}') \phi_k^K(\mathbf{r}')^* \phi_l^L(\mathbf{r}') d\mathbf{r} d\mathbf{r}'. \quad (3)$$

For practical calculations, one usually defines the Hubbard U and the Hund’s exchange parameter J by suitably averaging over matrix elements belonging to a single site. Here we use the Slater parametrization, which is often employed in DFT+ U calculations using the full d shell [5], where U is defined as average over both inter- and intra-orbital matrix elements (see, *e.g.*, [59]):

$$U_{\text{cRPA}}^I = \frac{1}{M^2} \sum_{ij} (W^{\mathcal{R}})_{ijjj}^{IIII}, \quad (4)$$

$$U_{\text{cRPA}}^I - J_{\text{cRPA}}^I = \frac{1}{M(M-1)} \sum_{ij} [(W^{\mathcal{R}})_{ijjj}^{IIII} - (W^{\mathcal{R}})_{ijji}^{IIII}]. \quad (5)$$

Here, M is the number of interacting orbitals on site I . We note that DFT+DMFT calculations sometimes employ the so-called Kanamori parametrization, where U is defined as average over only the inter-orbital matrix elements, *i.e.*, as $\frac{1}{M} \sum_i (W^{\mathcal{R}})_{iiii}^{IIII}$, which is larger than U_{cRPA}^I defined in Eq. (4) by about $\frac{8}{7} J_{\text{cRPA}}^I$ [42]. On the other hand, LRT is typically discussed in the context of a further simplified form of the interaction tensor introduced by Dudarev *et al.* [6], with a single effective Hubbard parameter which can be identified as $U_{\text{eff}} = U - J$, with U and J corresponding to the Slater parametrization. Accordingly, in this work, we will compare U_{LRT} with both U_{cRPA} as well as with $U_{\text{cRPA}} - J_{\text{cRPA}}$.

We focus on two different materials: KCuF₃ and Sr₂FeO₄. KCuF₃ has been studied using both DFT+ U and DFT+DMFT [5, 60], due to its Jahn-Teller-distorted structure and associated orbital order. For the purpose of this work, we consider KCuF₃ in the high symmetry cubic perovskite structure [shown in Fig. 1(a)], both for ease of computation and because it exhibits the prototypical band structure of a transition metal (TM) perovskite, with a clear separation between bands with dominant Cu d and F p character [see Fig. 1(b)]. Sr₂FeO₄ crystallizes in a layered perovskite structure [shown in Fig. 1(a)] [61, 62], and is of interest due to its structural and electronic similarity to the unconventional superconductor Sr₂RuO₄ [42]. The corresponding KS bands [see Fig. 1(c)] exhibit a small overlap between bands with dominant Fe d and dominant O p character. As reported recently, the computed value of U_{cRPA} for the Fe d states is too small to reproduce the experimentally observed insulating state of Sr₂FeO₄ within DFT+DMFT [42].

For both materials, we compare three different choices of the interacting subspace. In each case we represent the corresponding basis orbitals as MLWFs constructed from the KS band structures shown in Fig. 1, obtained

¹ In some cases, a different subdivision of the Hilbert space has been used to define the screening subspace within cRPA and to define the interacting subspace orbitals [50]. Here, we always use an identical subdivision to define both screening and interacting subspace.

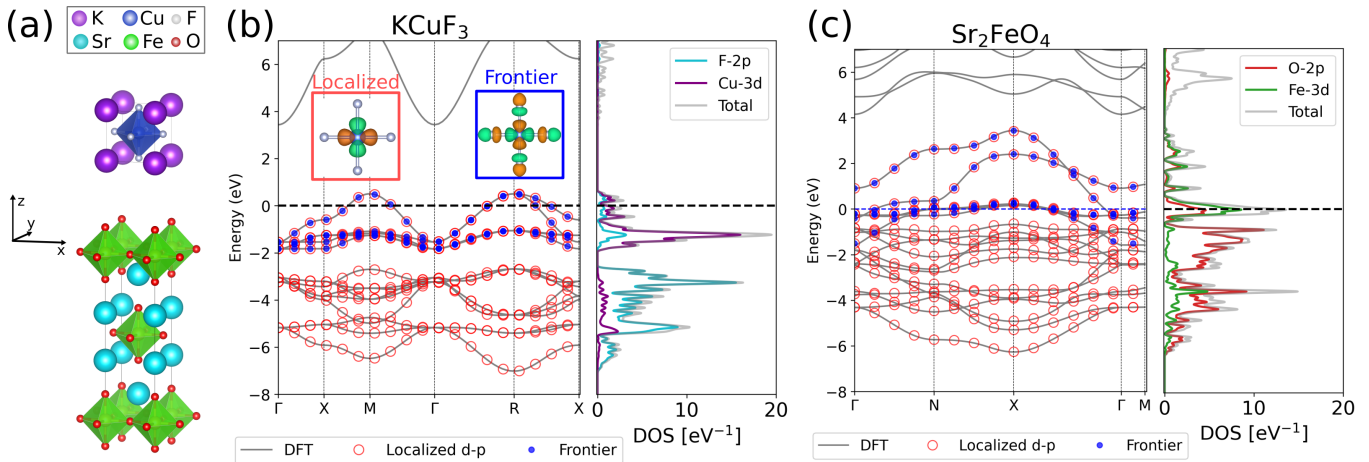


FIG. 1. (a) Crystal structures of cubic KCuF_3 and tetragonal Sr_2FeO_4 . (b) and (c) Band structure and projected densities of states (DOS) of (b) KCuF_3 and (c) Sr_2FeO_4 . Zero energy corresponds to the Fermi level. Open and closed circles indicate the bands recalculated from the localized $d-p$ and frontier orbital basis sets, respectively. The red and blue insets in (b) show isosurface plots of the Cu $d_{x^2-y^2}$ MLWF in the localized $d-p$ and frontier orbital basis sets, respectively.

for the nonmagnetic, *i.e.*, spin-degenerate, state. In the first case, we consider all bands with dominant TM d and ligand p character [see the projected densities of states in Fig. 1(b) and (c)], which are completely separated from other bands at lower and higher energies for both materials, and construct a complete MLWF basis for these bands consisting of five TM centered orbitals and three ligand centered orbitals per F or O within the unit cell. The resulting MLWFs closely resemble atomic d and p orbitals, respectively [see inset in Fig. 1(b) for the example of the Cu $d_{x^2-y^2}$ -like orbital in KCuF_3]. We call this the *localized $d-p$* basis. In the second case, we consider the same set of bands but construct only five MLWFs centered at the TM sites. These MLWFs again closely resemble atomic d orbitals but are slightly more localized compared to the $d-p$ basis. We call this second case *localized d -only*. Finally, in the third case, we restrict the energy window for the calculation of the MLWFs to include only the “frontier” bands with dominant TM d character immediately around the Fermi level. This results in five more delocalized d -like MLWFs, centered at the TM sites but exhibiting p -like tails at the surrounding ligand sites, which reflects the hybridized character of the corresponding bands [see the blue inset of Fig. 1(b) for the Cu $d_{x^2-y^2}$ -like orbital in KCuF_3]. We call this the *frontier orbital* basis. Such orbitals are often used in DFT+DMFT calculations.

In Fig. 2, we summarize the calculated values for U_{LRT} , U_{cRPA} , and $U_{\text{cRPA}} - J_{\text{cRPA}}$ for both KCuF_3 (a) and Sr_2FeO_4 (b) and the three different choices for the interacting subspace. We first focus on the localized $d-p$ and the frontier orbital basis, which completely span the KS bands within the respective energy windows [see Fig. 1 (b) and (c)]. The interaction parameters obtained with LRT (shown in blue) are quantitatively rather similar to those obtained with cRPA. This holds for both basis sets

and for both materials. Best agreement is typically observed between U_{LRT} and $U_{\text{cRPA}} - J_{\text{cRPA}}$, which supports the notion that U_{LRT} should be viewed as effective $U - J$. The agreement is particularly good for the localized $d-p$ basis, for which U_{LRT} and $U_{\text{cRPA}} - J_{\text{cRPA}}$ differ by less than 3%, except for the F site in KCuF_3 . For the frontier case the difference is somewhat larger, around 12%. The large difference between U_{LRT} and $U_{\text{cRPA}} - J_{\text{cRPA}}$ for the F p states in KCuF_3 in the $d-p$ basis, can be explained by the known tendency of LRT to overestimate U in cases with essentially completely full (or completely empty) shells, where the applicability of the linear response approach becomes problematic [7, 43, 63]. Indeed, the occupation of the F p states in KCuF_3 is nearly 0.99 electrons per orbital in our $d-p$ basis, while in Sr_2FeO_4 , the stronger hybridization with the TM d states reduces the average occupation of the O p states to ~ 0.91 , such that the applicability of LRT is unproblematic.

To better understand the good quantitative agreement as well as the remaining differences between LRT and cRPA for the frontier and localized $d-p$ cases, one can introduce a more general response tensor describing the full orbital-resolved response to a general non-local orbital-dependent perturbation [7]. As pointed out in [7], the LRT susceptibility can be viewed as a coarse-grained version of this generalized response tensor. One can further show (see the supplementary material [64] for full details), that for cases where the interacting subspace can be identified with a completely isolated set of bands, the bare cRPA susceptibility, $\chi_0^{\mathcal{R}}$, becomes equivalent to the generalized bare susceptibility restricted to the interacting subspace. If one then neglects the exchange-correlation contribution to the full susceptibility, which is included in LRT and in the generalized response function but is neglected in cRPA, U_{LRT} can be related to the cRPA interaction tensor from Eq. (3) through the

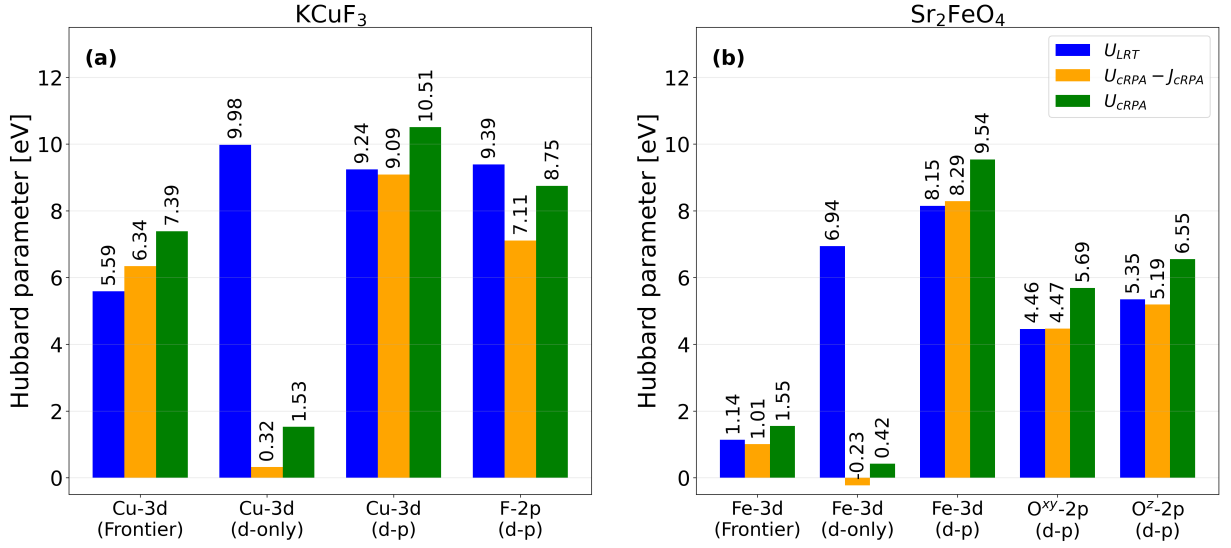


FIG. 2. Interaction parameters obtained from LRT and cRPA for (a) $KCuF_3$ and (b) Sr_2FeO_4 using different choices for the Hubbard projectors (frontier, localized d -only and d - p). Blue, orange, and green columns correspond to U_{LRT} , $U_{CRPA} - J_{CRPA}$, and U_{CRPA} , respectively. For Sr_2FeO_4 , O^{xy} refers to the oxygen within the Fe planes, while O^z refers to the apical oxygen.

expression:

$$U_{LRT}^I = \sum_{zt} \sum_{opqs}^{OPQS} (\tilde{\chi}_0^{-1})^{IZ} \left[(\chi_0)_{zzpo}^{ZZPO} (W^{\mathcal{R}})_{opqs}^{OPQS} \chi_{sqtt}^{SQTT} \right] (\tilde{\chi}^{-1})^{TI}. \quad (6)$$

Here, χ_0 and χ refer to the generalized susceptibilities, expressed in the orbital basis corresponding to the interacting subspace, while $\tilde{\chi}_0$ and $\tilde{\chi}$ refer to the coarse-grained LRT susceptibility matrices, with $\tilde{\chi}^{IR} = \sum_{ir} \chi_{iirr}^{IIRR}$ [7]. Rearranging the terms in Eq. (6), allows to write $U_{LRT}^I = U_{CRPA}^I + \Delta U^I$, where U_{CRPA} arises from isolating terms containing only bi-diagonal components of the generalized susceptibility tensor (i.e., elements of the form χ_{sstt}^{SSTT}) and replacing $(W^{\mathcal{R}})_{ppss}^{PPSS}$ with orbital averages defined analogous to Eq. (4) (see [64]). ΔU^I contains all other contributions arising from elements of the generalized susceptibility tensor that are not purely bi-diagonal. These include local exchange terms containing matrix elements of the form $(W^{\mathcal{R}})_{oppo}^{OOOO}$, as well as additional on-site and inter-site off-diagonal terms associated with particle-hole excitations within the interacting subspace that are excluded within cRPA.

To summarize, for the case of an isolated interacting subspace, and if the exchange correlation contribution to the response is neglected, U_{LRT} is equal to U_{CRPA} plus all the additional terms included in ΔU . The overall good quantitative agreement between LRT and cRPA for the frontier and d - p subspaces indicate that, at least for the materials considered here, these differences are small, in particular if the local exchange terms in Eq. (6) are taken into account in an effective way by considering $U_{CRPA} - J_{CRPA}$. However, we also note that test calcula-

tions where we removed the exchange-correlation part of the response within LRT led to an increase of U_{LRT} by about 5-10%, depending on the specific case. This shows that both this effect as well as the additional terms in Eq. (6) can contribute notably to the difference between U_{LRT} and U_{CRPA} .

Lastly, we discuss the localized d -only case (second set of columns in both panels of Fig. 2), for which LRT and cRPA lead to drastically different results. Both U_{CRPA} and $U_{CRPA} - J_{CRPA}$ are very small in this case, with the latter even taking negative values for Sr_2FeO_4 . In contrast, U_{LRT} is much larger and comparable to the values obtained for the localized d - p basis.

The very small values for U_{CRPA} and $U_{CRPA} - J_{CRPA}$ obtained for the d -only case are related to the strong hybridization between the interacting and screening subspaces in the underlying bands. Several methods have been suggested to obtain $\chi_0^{\mathcal{R}}$ in such cases [48, 65, 66]. Here, we use the method introduced in Ref. [65], which assigns weights to each particle-hole transition in Eq. (2) according to the product of the weights of the \mathcal{D} subspace in the corresponding Bloch functions. For bands with mixed character that are close to or even crossing the Fermi level, this can lead to transitions with very low energy which contribute strongly to the screening and thus lead to a very small U_{CRPA} .² This behavior is closely related to the general tendency of cRPA to overscreen [68–71],

² We note that even though the “projector method” [66] (not implemented in RESPACK) typically results in larger interaction parameters compared to the “weighted method” (see, e.g., [59, 67]), it nevertheless suffers from the same problem of very low energy transitions and a resulting overscreening [59].

which is strongest if the interacting and screening subspaces are close in energy, such that corrections beyond RPA become important [68]. The d -only case thus represents a problematic case, where the general applicability of the cRPA approach becomes questionable, and the results can furthermore depend sensitively on the specific way the two subspaces are separated. On the other hand, the d -only case is quite relevant for practical applications, since in DFT+ U and DFT+DMFT calculations for TM compounds, one typically applies the U correction only on the TM sites, while the ligand states are considered as weakly interacting. Interestingly, it was recently noted that explicitly considering interaction effects also on the ligands can in fact improve the quantitative description of various TM compounds [72].

Within LRT, apart from the fact that the d -only MLWFs are slightly more localized, the main difference to the d - p case is the absence of TM–ligand off-diagonal elements in the susceptibility matrices $\tilde{\chi}^{IJ}$ and $\tilde{\chi}_0^{IJ}$, which affect U_{LRT}^I due to the inversion in Eq. (1). These off-diagonal elements are larger in Sr_2FeO_4 than in KCuF_3 , due to the stronger d - p hybridization in the oxide compared to the more ionic fluoride, which results in a larger difference of U_{LRT} between the two localized basis sets for Sr_2FeO_4 . However, even though the very strong overscreening observed in cRPA for the d -only case seems to be absent in LRT, we note that, since the generalized susceptibility $(\chi_0)_{ijkl}^{IJKL}$ is equivalent to the bare cRPA susceptibility [64], the general overscreening effects identified for cRPA [68–71] can be expected to also affect U_{LRT} , even though the practical problem of how to separate two strongly hybridized subspaces does not appear. This could explain why, in the case of Sr_2FeO_4 , for which the frontier bands overlap slightly with the lower-lying screening bands, both U_{LRT} and $U_{\text{cRPA}} - J_{\text{cRPA}}$ in the frontier basis are too low to reproduce the experimentally observed insulating state [42].

In summary, we have incorporated the use of Wannier functions as Hubbard projectors in LRT calculation of the Hubbard U , enabling a direct quantitative compar-

ison with corresponding cRPA calculations. Our numerical results show that in cases where the interacting subspace corresponds to an isolated set of bands, both LRT and cRPA yield comparable but not identical Hubbard parameters. We further showed, that the quantitative agreement can be understood also on a formal level, since both methods are based on similar approximations. Differences arise from neglecting the change of the exchange-correlation potential in the cRPA response and the fact that LRT takes into account additional screening effects related to local exchange as well as inter-site and inter-orbital contributions within the interacting subspace.

For cases where the interacting and screening subspaces are strongly hybridized and do not correspond to a separated set of bands, we find that cRPA can produce unphysically small interaction values, questioning its applicability in such cases. While U_{LRT} appears unaffected by this problem, the fact that LRT does not systematically exclude screening within the interacting subspace could lead to a “double-counting” in the subsequent treatment of interaction effects within the interacting subspace.

Finally, we point out that using well-defined Wannier projectors not only allows for a systematic comparison between LRT and cRPA (and potentially other methods to calculate U), but also offers greater transferability across different implementations. This can help to remedy the large spread in reported U values used for the same materials but obtained with different DFT codes and potentially different subspace definitions.

We are thankful to Matteo Cococcioni and Kazuma Nakamura for valuable discussions. This research was supported by ETH Zürich. The Flatiron Institute is a division of the Simons Foundation. I.T. acknowledges partial support by the NCCR MARVEL, a National Centre of Competence in Research, funded by the Swiss National Science Foundation (Grant number 205602). Calculations were performed on the “Euler” cluster of ETH Zürich.

-
- [1] B. Keimer and J. E. Moore, The physics of quantum materials, *Nature Physics* **13**, 1045 (2017).
 - [2] P. Hohenberg and W. Kohn, Inhomogeneous electron gas, *Phys. Rev.* **136**, B864 (1964).
 - [3] W. Kohn and L. Sham, Self-consistent equations including exchange and correlation effects, *Phys. Rev.* **140**, A1133 (1965).
 - [4] V. I. Anisimov, J. Zaanen, and O. K. Andersen, Band theory and Mott insulators: Hubbard U instead of Stoner I , *Physical Review B* **44**, 943 (1991).
 - [5] A. Liechtenstein, V. Anisimov, and J. Zaanen, Density-functional theory and strong interactions: Orbital ordering in Mott-Hubbard insulators, *Phys. Rev. B* **52**, R5467 (1995).
 - [6] S. L. Dudarev, G. A. Botton, S. Y. Savrasov, C. J. Humphreys, and A. P. Sutton, Electron-energy-loss spectra and the structural stability of nickel oxide: An LSDA+ U study, *Physical Review B* **57**, 1505 (1998).
 - [7] B. Himmetoglu, A. Floris, S. de Gironcoli, and M. Cococcioni, Hubbard-corrected DFT energy functionals: The LDA+ U description of correlated systems, *International Journal of Quantum Chemistry* **114**, 14 (2013).
 - [8] G. Georges, A. amd Kotliar, W. Krauth, and M. J. Rozenberg, Dynamical mean-field theory of strongly correlated fermion systems and the limit of infinite dimensions, *Rev. Mod. Phys.* **68**, 13 (1996).
 - [9] G. Kotliar, S. Y. Savrasov, K. Haule, V. S. Oudovenko, O. Parcollet, and C. A. Marianetti, Electronic structure calculations with dynamical mean-field theory, *Reviews of Modern Physics* **78**, 865 (2006).

- [10] K. Held, Electronic structure calculations using dynamical mean field theory, *Advances in Physics* **56**, 829 (2007).
- [11] V. L. Campo and M. Cococcioni, Extended DFT + U + V method with on-site and inter-site electronic interactions, *Journal of Physics: Condensed Matter* **22**, 055602 (2010).
- [12] P. Dederichs, S. Blügel, R. Zeller, and H. Akai, Ground States of Constrained Systems: Application to Cerium Impurities, *Phys. Rev. Lett.* **53**, 2512 (1984).
- [13] A. McMahan, R. Martin, and S. Satpathy, Calculated effective Hamiltonian for La_2CuO_4 and solution in the impurity Anderson approximation, *Phys. Rev. B* **38**, 6650 (1988).
- [14] O. Gunnarsson, O. Andersen, O. Jepsen, and J. Zaanen, Density-functional calculation of the parameters in the Anderson model: Application to Mn in CdTe, *Phys. Rev. B* **39**, 1708 (1989).
- [15] M. Hybertsen, M. Schlüter, and N. Christensen, Calculation of Coulomb-interaction parameters for La_2CuO_4 using a constrained-density-functional approach, *Phys. Rev. B* **39**, 9028 (1989).
- [16] O. Gunnarsson, Calculation of parameters in model Hamiltonians, *Phys. Rev. B* **41**, 514 (1990).
- [17] W. Pickett, S. Erwin, and E. Ethridge, Reformulation of the LDA+U method for a local-orbital basis, *Phys. Rev. B* **58**, 1201 (1998).
- [18] I. Solovyev and M. Imada, Screening of Coulomb interactions in transition metals, *Phys. Rev. B* **71**, 045103 (2005).
- [19] K. Nakamura, R. Arita, Y. Yoshimoto, and S. Tsuneyuki, First-principles calculation of effective onsite Coulomb interactions of 3d transition metals: Constrained local density functional approach with maximally localized Wannier functions, *Phys. Rev. B* **74**, 235113 (2006).
- [20] M. Shishkin and H. Sato, Self-consistent parametrization of DFT+U framework using linear response approach: Application to evaluation of redox potentials of battery cathodes, *Phys. Rev. B* **93**, 085135 (2016).
- [21] M. Cococcioni and S. de Gironcoli, Linear response approach to the calculation of the effective interaction parameters in the $\text{LDA}+\text{U}$ method, *Physical Review B* **71**, 035105 (2005).
- [22] I. Timrov, N. Marzari, and M. Cococcioni, Hubbard parameters from density-functional perturbation theory, *Physical Review B* **98**, 085127 (2018).
- [23] E. B. Linscott, D. J. Cole, M. C. Payne, and D. D. O'Regan, Role of spin in the calculation of Hubbard U and Hund's J parameters from first principles, *Physical Review B* **98**, 235157 (2018).
- [24] I. Timrov, N. Marzari, and M. Cococcioni, Self-consistent Hubbard parameters from density-functional perturbation theory in the ultrasoft and projector-augmented wave formulations, *Physical Review B* **103**, 045141 (2021).
- [25] I. Timrov, N. Marzari, and M. Cococcioni, HP – A code for the calculation of Hubbard parameters using density-functional perturbation theory, *Computer Physics Communications* **279**, 108455 (2022).
- [26] E. Macke, I. Timrov, N. Marzari, and L. C. Ciacchi, Orbital-Resolved DFT+U for Molecules and Solids, *Journal of Chemical Theory and Computation* **20**, 4824–4843 (2024).
- [27] N. Mosey and E. Carter, Ab initio evaluation of Coulomb and exchange parameters for DFT+U calculations, *Phys. Rev. B* **76**, 155123 (2007).
- [28] N. Mosey, P. Liao, and E. Carter, Rotationally invariant ab initio evaluation of Coulomb and exchange parameters for DFT+U calculations, *J. Chem. Phys.* **129**, 014103 (2008).
- [29] A. Andriotis, R. Sheetz, and M. Menon, LSDA+U method: A calculation of the U values at the Hartree-Fock level of approximation, *Phys. Rev. B* **81**, 245103 (2010).
- [30] L. Agapito, S. Curtarolo, and M. Buongiorno Nardelli, Reformulation of DFT+U as a Pseudohybrid Hubbard Density Functional for Accelerated Materials Discovery, *Phys. Rev. X* **5**, 011006 (2015).
- [31] N. Tancogne-Dejean and A. Rubio, Parameter-free hybridlike functional based on an extended Hubbard model: DFT+U+V, *Phys. Rev. B* **102**, 155117 (2020).
- [32] S.-H. Lee and Y.-W. Son, First-principles approach with a pseudohybrid density functional for extended Hubbard interactions, *Phys. Rev. Research* **2**, 043410 (2020).
- [33] M. Springer and F. Aryasetiawan, Frequency-dependent screened interaction in Ni within the random-phase approximation, *Phys. Rev. B* **57**, 4364 (1998).
- [34] T. Kotani, *Ab initio* random-phase-approximation calculation of the frequency-dependent effective interaction between 3d electrons: Ni, Fe, and MnO, *J. Phys.: Condens. Matter* **12**, 2413 (2000).
- [35] F. Aryasetiawan, M. Imada, A. Georges, G. Kotliar, S. Biermann, and A. I. Lichtenstein, Frequency-dependent local interactions and low-energy effective models from electronic structure calculations, *Physical Review B* **70**, 195104 (2004).
- [36] F. Aryasetiawan, K. Karlsson, O. Jepsen, and U. Schönberger, Calculations of Hubbard U from first-principles, *Physical Review B* **74**, 125106 (2006).
- [37] N. E. Kirchner-Hall, W. Zhao, Y. Xiong, I. Timrov, and I. Dabo, Extensive Benchmarking of DFT+U Calculations for Predicting Band Gaps, *Applied Sciences* **11**, 2395 (2021).
- [38] M. Capdevila-Cortada, Z. Łodziana, and N. López, Performance of DFT+U Approaches in the Study of Catalytic Materials, *ACS Catalysis* **6**, 8370 (2016).
- [39] G. C. Moore, M. K. Horton, E. Linscott, A. M. Ganose, M. Siron, D. D. O'Regan, and K. A. Persson, High-throughput determination of Hubbard U and Hund J values for transition metal oxides via the linear response formalism, *Physical Review Materials* **8**, 014409 (2024).
- [40] P. Seth, O. E. Peil, L. Pourovskii, M. Betzinger, C. Friedrich, O. Parcollet, S. Biermann, F. Aryasetiawan, and A. Georges, Renormalization of effective interactions in a negative charge transfer insulator, *Physical Review B* **96**, 205139 (2017).
- [41] J. Souto-Casares, N. A. Spaldin, and C. Ederer, Oxygen vacancies in strontium titanate: A $\text{DFT}+\text{DMFT}$ study, *Physical Review Research* **3**, 023027 (2021).
- [42] A. Kazemi-Moridani, S. Beck, A. Hampel, A.-M. S. Tremblay, M. Côté, and O. Gingras, Strontium ferrite under pressure: Potential analog to strontium ruthenate, *Physical Review B* **109**, 165146 (2024).
- [43] R. Tesch and P. M. Kowalski, Hubbard U parameters for transition metals from first principles, *Physical Review B* **105**, 195153 (2022).
- [44] B.-L. Liu, Y.-C. Wang, Y. Liu, Y.-J. Xu, X. Chen, H.-Z. Song, Y. Bi, H.-F. Liu, and H.-F. Song, Comparative

- study of first-principles approaches for effective Coulomb interaction strength U_{eff} between localized f -electrons: Lanthanide metals as an example, *J. Chem. Phys.* **158**, 084108 (2023).
- [45] A. Carta, I. Timrov, P. Mlkvik, A. Hampel, and C. Ederer, Explicit demonstration of the equivalence between DFT + U and the Hartree-Fock limit of DFT + DMFT, *Physical Review Research* **7**, 013289 (2025).
- [46] R. Mahajan, I. Timrov, N. Marzari, and A. Kashyap, Importance of intersite Hubbard interactions in β -MnO₂: A first-principles DFT+U+V study, *Phys. Rev. Mat.* **5**, 104402 (2021).
- [47] O. Bengone, M. Alouani, P. Blöchl, and J. Hugel, Implementation of the projector augmented-wave LDA+U method: Application to the electronic structure of NiO, *Physical Review B* **62**, 16392 (2000).
- [48] T. Miyake, F. Aryasetiawan, and M. Imada, Ab initio procedure for constructing effective models of correlated materials with entangled band structure, *Physical Review B* **80**, 155134 (2009).
- [49] R. Sakuma and F. Aryasetiawan, First-principles calculations of dynamical screened interactions for the transition metal oxides MMO ($\text{M}=\text{Mn, Fe, Co, Ni}$), *Physical Review B* **87**, 165118 (2013).
- [50] T. Miyake, L. Pourovskii, V. Vildosola, S. Biermann, and A. Georges, D- and f-Orbital Correlations in the REFeAsO Compounds, *Journal of the Physical Society of Japan* **77**, 99 (2008).
- [51] T. Miyake and F. Aryasetiawan, Screened Coulomb interaction in the maximally localized Wannier basis, *Physical Review B* **77**, 085122 (2008).
- [52] P. Giannozzi, S. Baroni, N. Bonini, M. Calandra, R. Car, C. Cavazzoni, D. Ceresoli, G. L. Chiarotti, M. Cococcioni, I. Dabo, A. D. Corso, S. de Gironcoli, S. Fabris, G. Fratesi, R. Gebauer, U. Gerstmann, C. Gougoussis, A. Kokalj, M. Lazzeri, L. Martin-Samos, N. Marzari, F. Mauri, R. Mazzarello, S. Paolini, A. Pasquarello, L. Paulatto, C. Sbraccia, S. Scandolo, G. Sclauzero, A. P. Seitsonen, A. Smogunov, P. Umari, and R. M. Wentzcovitch, QUANTUM ESPRESSO: A modular and open-source software project for quantum simulations of materials, *Journal of Physics: Condensed Matter* **21**, 395502 (2009).
- [53] P. Giannozzi, O. Andreussi, T. Brumme, O. Bunau, M. B. Nardelli, M. Calandra, R. Car, C. Cavazzoni, D. Ceresoli, M. Cococcioni, N. Colonna, I. Carnimeo, A. D. Corso, S. de Gironcoli, P. Delugas, R. A. DiStasio, A. Ferretti, A. Floris, G. Fratesi, G. Fugallo, R. Gebauer, U. Gerstmann, F. Giustino, T. Gorni, J. Jia, M. Kawamura, H.-Y. Ko, A. Kokalj, E. Küçükbenli, M. Lazzeri, M. Marsili, N. Marzari, F. Mauri, N. L. Nguyen, H.-V. Nguyen, A. Otero-de-la-Roza, L. Paulatto, S. Poncé, D. Rocca, R. Sabatini, B. Santra, M. Schlipf, A. P. Seitsonen, A. Smogunov, I. Timrov, T. Thonhauser, P. Umari, N. Vast, X. Wu, and S. Baroni, Advanced capabilities for materials modelling with Quantum ESPRESSO, *Journal of Physics: Condensed Matter* **29**, 465901 (2017).
- [54] P. Giannozzi, O. Baseggio, P. Bonfà, D. Brunato, R. Car, I. Carnimeo, C. Cavazzoni, S. de Gironcoli, P. Delugas, F. Ferrari Ruffino, A. Ferretti, N. Marzari, I. Timrov, A. Urru, and S. Baroni, Quantum ESPRESSO toward the exascale, *J. Chem. Phys.* **152**, 154105 (2020).
- [55] G. Pizzi, V. Vitale, R. Arita, S. Blügel, F. Freimuth, G. Géranton, M. Gibertini, D. Gresch, C. Johnson, T. Koretsune, J. Ibañez-Azpiroz, H. Lee, J.-M. Lihm, D. Marchand, A. Marrazzo, Y. Mokrousov, J. I. Mustafa, Y. Nohara, Y. Nomura, L. Paulatto, S. Poncé, T. Ponweiser, J. Qiao, F. Thöle, S. S. Tsirkin, M. Wierzbowska, N. Marzari, D. Vanderbilt, I. Souza, A. A. Mostofi, and J. R. Yates, Wannier90 as a community code: New features and applications, *Journal of Physics: Condensed Matter* **32**, 165902 (2020).
- [56] N. Marzari, A. A. Mostofi, J. R. Yates, I. Souza, and D. Vanderbilt, Maximally localized Wannier functions: Theory and applications, *Rev. Mod. Phys.* **84**, 1419 (2012).
- [57] K. Nakamura, Y. Yoshimoto, Y. Nomura, T. Tadano, M. Kawamura, T. Kosugi, K. Yoshimi, T. Misawa, and Y. Motoyama, RESPACK: An *ab initio* tool for derivation of effective low-energy model of material, *Computer Physics Communications* **261**, 107781 (2021).
- [58] K. Kurita, T. Misawa, K. Yoshimi, K. Ido, and T. Koretsune, Interface tool from Wannier90 to RESPACK: Wan2respack, *Computer Physics Communications* **292**, 108854 (2023).
- [59] M. E. Merkel and C. Ederer, Calculation of screened Coulomb interaction parameters for the charge-disproportionated insulator CaFeO₃, *Physical Review Research* **6**, 013230 (2024).
- [60] E. Pavarini, E. Koch, and A. I. Lichtenstein, Mechanism for orbital ordering in KCuF₃, *Physical Review Letters* **101**, 266405 (2008).
- [61] S. E. Dann, M. T. Weller, D. B. Currie, M. F. Thomas, and A. D. Al-Rawwas, Structure and magnetic properties of Sr₂FeO₄ and Sr₃Fe₂O₇ studied by powder neutron diffraction and Mössbauer spectroscopy, *Journal of Materials Chemistry* **3**, 1231 (1993).
- [62] S. E. Dann, M. T. Weller, and D. B. Currie, The synthesis and structure of Sr₂FeO₄, *Journal of Solid State Chemistry* **92**, 237 (1991).
- [63] K. Yu and E. A. Carter, Communication: Comparing *ab initio* methods of obtaining effective U parameters for closed-shell materials, *The Journal of Chemical Physics* **140**, 121105 (2014).
- [64] See the supplementary information provided with this article.
- [65] E. Şaşıoğlu, C. Friedrich, and S. Blügel, Effective Coulomb interaction in transition metals from constrained random-phase approximation, *Physical Review B* **83**, 121101 (2011).
- [66] M. Kaltak, *Merging GW with DMFT*, Ph.D. thesis, University of Vienna (2015).
- [67] I. R. Reddy, M. Kaltak, and B. Kim, Unveiling the cRPA: A Comparative Analysis of Methods for Calculating Hubbard Parameters [10.48550/ARXIV.2503.11142](https://arxiv.org/abs/10.48550/ARXIV.2503.11142) (2025).
- [68] E. G. C. P. van Loon, M. Rösner, M. I. Katsnelson, and T. O. Wehling, Random phase approximation for gapped systems: Role of vertex corrections and applicability of the constrained random phase approximation, *Physical Review B* **104**, 045134 (2021).
- [69] C. Honerkamp, H. Shinaoka, F. F. Assaad, and P. Werner, Limitations of constrained random phase approximation downfolding, *Physical Review B* **98**, 235151 (2018).
- [70] P. Werner and M. Casula, Dynamical screening in correlated electron systems—from lattice models to realistic materials, *Journal of Physics: Condensed Matter* **28**, 383001 (2016).

- [71] H. Shinaoka, M. Troyer, and P. Werner, Accuracy of downfolding based on the constrained random-phase approximation, *Physical Review B* **91**, 245156 (2015).
- [72] A. Carta, A. Panda, and C. Ederer, Importance of ligand on-site interactions for the description of Mott-insulators in DFT+DMFT [10.48550/ARXIV.2502.17229](#) (2025).